MOLECULAR AND CELLULAR BIOLOGY, Feb. 2011, p. 430–441 Vol. 31, No. 3
0270-7306/11/$12.00 doi:10.1128/MCB.00983-10

Insulin Receptor Substrates Irs1 and Irs2 Coordinate Skeletal Muscle Growth and Metabolism via the Akt and AMPK Pathways[▽]

Yun Chau Long,[1]† Zhiyong Cheng,[2] Kyle D. Copps,[1,2] and Morris F. White[1,2]*

Howard Hughes Medical Institute[1] and Division of Endocrinology,[2] Children's Hospital Boston, Harvard Medical School, Boston, Massachusetts 02115

Received 22 August 2010/Returned for modification 17 September 2010/Accepted 21 November 2010

Coordination of skeletal muscle growth and metabolism with nutrient availability is critical for metabolic homeostasis. To establish the role of insulin-like signaling in this process, we used muscle creatine kinase (MCK)-Cre to disrupt expression of insulin receptor substrates Irs1 and Irs2 in mouse skeletal/cardiac muscle. In 2-week-old mice, skeletal muscle masses and insulin responses were slightly affected by Irs1, but not Irs2, deficiency. In contrast, the combined deficiency of Irs1 and Irs2 (MDKO mice) severely reduced skeletal muscle growth and Akt→mTOR signaling and caused death by 3 weeks of age. Autopsy of MDKO mice revealed dilated cardiomyopathy, reflecting the known requirement of insulin-like signaling for cardiac function (P. G. Laustsen et al., Mol. Cell. Biol. 27:1649-1664, 2007). Impaired growth and function of MDKO skeletal muscle were accompanied by increased Foxo-dependent atrogene expression and amino acid release. MDKO mice were resistant to injected insulin, and their isolated skeletal muscles showed decreased insulin-stimulated glucose uptake. Glucose utilization in MDKO mice and isolated skeletal muscles was shifted from oxidation to lactate production, accompanied by an elevated AMP/ATP ratio that increased AMP-activated protein kinase (AMPK)→acetyl coenzyme A carboxylase (ACC) phosphorylation and fatty acid oxidation. Thus, insulin-like signaling via Irs1/2 is essential to terminate skeletal muscle catabolic/fasting pathways in the presence of adequate nutrition.

Skeletal muscle is a major site of bodily energy consumption, so the capacity to coordinate its growth and metabolism with nutrient availability is critical for survival (5, 19). Insulin-like signaling—mediated by insulin and insulin-like growth factor I (IGF1)—integrates animal growth, metabolism, and life span (55) and plays an essential role in cardiac function (35). The receptors for insulin and IGF1 (Ir and Igf1r, respectively) activate common intracellular signaling cascades but display distinct biological functions: *Ir* knockout mice are slightly small at birth and die after a few days, owing to extreme hyperglycemia and ketoacidosis; *Igf1r* knockout mice are 50% smaller than normal and die after birth from severe developmental defects (37). Many studies suggest that metabolic disease, including diabetes, originates from dysregulated skeletal muscle insulin action (45, 48). Unlike liver and adipose tissues, which express exclusively insulin receptors, skeletal muscle expresses both Ir and Igf1r (35). Deficiency of Ir or Igf1r in mouse skeletal and cardiac muscle has minor effects upon glucose homeostasis and muscle function (37); glucose tolerance in young mice lacking both receptors in skeletal and cardiac muscle is also nearly normal, until they die suddenly owing to dilated cardiomyopathy (35).

The insulin and IGF1 receptors are tyrosine kinases that phosphorylate various proteins, including the insulin receptor substrates Irs1 and Irs2. Irs1 and Irs2 are usually expressed together in all cells and tissues; however, they can display distinct signaling functions in specific cellular contexts (29). In mouse liver, where both of the Irs proteins mediate insulin action, Irs1 generates a persistent signal in the postprandial state, whereas Irs2 might be more important during fasting and immediately after eating (22, 31). Irs2 is critical for pancreatic β-cell growth, function, and development, whereas Irs1 appears to contribute mainly to insulin secretory mechanisms (55). In the central nervous system, Irs2 signaling plays an important role in brain growth, nutrient sensing, and life span regulation, whereas Irs1 might to be less important for these functions (55). Previous cell-based experiments suggest that Irs1→Akt2 signaling plays an important role in myoblast differentiation and glucose metabolism, whereas Irs2→Akt1 signaling contributes to lipid metabolism (29). Whether Irs1 and Irs2 mediate distinct insulin and IGF1 receptor signaling in skeletal muscle is unknown.

During periods of nutrient abundance, insulin-like signaling stimulates the Akt→mTOR pathway in skeletal muscle, which increases amino acid uptake and promotes protein synthesis (5, 19). Akt also phosphorylates and inactivates Foxo transcription factors to decrease the expression of genes that promote muscle autophagy (60). Conversely, when the circulating insulin concentration is relatively low during fasting, skeletal muscle protein is degraded, and amino acids are released for use by other organs, including the liver for gluconeogenesis and acute phase protein synthesis (36, 42). Thus, the regulation of protein synthesis/degradation by insulin-like signaling coordinates growth and metabolism of skeletal muscle with nutrient availability to preserve interorgan energy homeostasis (50, 54).

Skeletal muscle has the capacity to utilize energy substrates selectively in response to changes in nutrient availability (14,

* Corresponding author. Mailing address: Howard Hughes Medical Institute, Division of Endocrinology, Children's Hospital Boston, Center for Life Sciences, CLS-16020, 3 Blackfan Circle, Boston, MA 02115. Phone: (617) 919-2846. Fax: (617) 730-0244. E-mail: morris.white@childrens.harvard.edu.

† Present address: Eli Lilly and Company, Indianapolis, IN 46225.

▽ Published ahead of print on 6 December 2010.

30). Skeletal muscle is a major site of glucose uptake and oxidation under insulin-stimulated conditions; however, during fasting, fatty acid is the predominant substrate for oxidation by skeletal muscle (14, 30). This metabolic flexibility spares carbohydrate for use in the brain and, given the substantial mass and energy expenditure of skeletal muscle, is an important attribute for energy homeostasis and survival. During prolonged starvation or exercise, the increase in the AMP/ATP ratio or depletion of glycogen stores activates the AMP-activated protein kinase (AMPK), which in turn stimulates skeletal muscle fatty acid oxidation via phosphorylation of its downstream target acetyl coenzyme A (acetyl-CoA) carboxylase (ACC) (27, 39). Although the intracellular energy level controls the AMPK→ACC axis, it is unclear how insulin-like signals modulate the AMPK pathway in skeletal muscle. Given their involvement in both IGF1 and insulin signaling, the adaptor proteins Irs1 and Irs2 provide a logical point of convergence for the coordination of skeletal muscle growth and metabolism. In this work, we show that insulin-like signals mediated by Irs1 and Irs2 are essential to preserve skeletal muscle mass and downregulate catabolic/fasting-type metabolism—even in the presence of adequate nutrition—by both activating Akt→mTOR signaling and limiting AMPK activation.

MATERIALS AND METHODS

Animals. Animal experiments were performed according to procedures approved by the Children's Hospital Boston Institutional Animal Care and Use Committee. The floxed Irs1 mice ($Irs1^{L/L}$) (13), floxed Irs2 mice ($Irs2^{L/L}$) (38), and muscle creatine kinase (MCK)-Cre mice (8) were intercrossed to generate muscle-specific Irs1 knockout (MKO1) mice, muscle-specific Irs2 knockout (MKO2) mice, or double-knockout (MDKO) mice on a C57BL/6 and 129Sv mixed background. These mice were maintained on regular chow (Prolab Isopro 5P76, with 14 kcal% of energy from fat of diverse sources).

Blood chemistry and body composition. Serum samples were analyzed for insulin and free fatty acids using commercial protocols and reagents. Blood glucose and lactate concentrations were measured using a portable glucometer (Bayer) and lactate meter (Lactate Scout), respectively. For glucose tolerance tests, mice were fasted for 6 h prior to intraperitoneal injections of 2 g D-glucose/kg body weight. For insulin tolerance tests, mice received intraperitoneal injections of 1 U of insulin/kg (Humulin; Eli Lilly). Body composition was assessed using a DEXA imaging station, according to the manufacturer's instructions (GE Healthcare). *In vivo* insulin stimulation in mice that were fasted and deeply anesthetized was carried out. Insulin (5 U/10 g) or its diluent was injected via the inferior vena cava. Skeletal muscles were collected 5 min after injection and frozen in liquid nitrogen. AMP and ATP concentration were analyzed by high-pressure liquid chromatography (HPLC) (Vanderbilt University), and glycogen content was determined by enzymatic assay (BioVision). The skeletal muscle cross-sectional area was determined using LSM software (Zeiss).

Muscle incubation. *Ex vivo* muscle incubation was performed as described previously (3). Incubation medium was prepared from stocks of gassed (95% O_2, 5%CO_2) Krebs-Henseleit buffer (KHB) supplemented with 5 mM HEPES and 0.1% bovine serum albumin (radioimmunoassay grade). Extensor digitorum longus (EDL) and soleus muscles were excised and incubated at 30°C in a shaking water bath under a constant gas phase (95% O_2/5% CO_2), unless stated otherwise. For glucose uptake, muscles were preincubated for 30 min in KHB containing 2 mM pyruvate in the absence or presence of 12 nM insulin. Muscles were then transferred to KHB with additions of 1 mM 2-deoxy-D-[1,2-^{3}H]glucose (2.5 μCi/ml) and 19 mM [U-^{14}C]mannitol (0.7 μCi/ml) for 20 min with or without insulin. Extracellular space and intracellular 2-deoxyglucose concentrations were determined by liquid scintillation counting of muscle lysate homogenized in 0.5 M NaOH. For palmitate oxidation, muscles were incubated for 2 h in Krebs-Henseleit buffer supplemented with 5 mM HEPES, 1.5% fatty acid-free bovine serum albumin, 5 mM glucose, and 0.5 mM [1-^{14}C]palmitate (1.0 μCi/ml). To measure glucose oxidation, muscles were incubated for 1 h in 0.5 ml of Krebs-Henseleit buffer containing 8 mM [U-^{14}C]glucose (0.3 μCi/ml). Vials were sealed with a rubber stopper that was fixed with a center well. After incubation, muscles were removed and snap-frozen with liquid nitrogen, 0.2 ml of 2 M NaOH was injected through the rubber stopper into the center well, and 0.2 ml of 75% perchloric acid was injected into the medium. Released CO_2 was collected for 2 h, and center wells were transferred to vials for liquid scintillation counting.

For the release of metabolites, muscles were incubated in KHB for an hour, and the amounts of lactate and amino acids in the media were assayed by using commercially available protocols and reagents (BioVision). Muscles were removed, and the media were frozen in liquid nitrogen. Muscles were homogenized in 0.5 M NaOH, and sample aliquots were used for protein determination using commercially available protocols and reagents (Bio-Rad). *Ex vivo* IGF1 stimulation was performed by incubating the muscles in KHB containing IGF1 (500 ng/ml) for 30 min, as described above.

Immunoblotting. Muscle samples (collected under random-fed conditions unless stated otherwise) were homogenized by a motor-driven pestle in 0.3 ml of ice-cold lysis buffer containing 20 mM Tris (pH 8.0), 137 mM NaCl, 2.7 mM KCl, 10 mM NaF, 1 mM MgCl, 1 mM Na_3VO_4, 0.2 mM phenylmethylsulfonyl fluoride, 10% glycerol, 1% Triton X-100, 1 μg/ml aprotinin, and 1 μg/ml leupeptin. Homogenates were solubilized by end-over-end mixing at 4°C for 60 min and subjected to centrifugation for 10 min at 12,000 × *g* at 4°C. Total protein was determined using commercially available protocols and reagents (Bio-Rad). Proteins (50 μg) solubilized in Laemmli sample buffer were separated by sodium dodecyl sulfate-polyacrylamide gel electrophoresis (SDS-PAGE) and transferred to Immobilon-P membranes (Millipore, Bedford, MA) (11). Immunoblotting was performed using antibodies against Irs1 and Irs2 (Millipore) and other proteins (Cell Signaling). The immunoblots were visualized by chemiluminescence (Bio-Rad), and the signal intensity was quantified by using densitometry (Kodak GL440 and Kodak molecular imaging software version 4.5.0).

Real-time PCR. RNA was purified with Trizol reagent (Sigma) and treated with DNase I, according to recommendations of the manufacturer (Ambion). DNase-treated RNA was used as a template for cDNA synthesis using the SuperScript first-strand synthesis system (Invitrogen). The quantity of cDNA for each transcript was measured using real-time PCR in a final volume of 25 μl, consisting of a diluted cDNA sample, 1× iQ SYBR green (Bio-Rad), primers optimized for each target gene, and nuclease-free water. Relative quantities of target transcripts were calculated from duplicate samples after normalization of the data against β-actin using the standard curve method.

RESULTS

Muscle-specific disruption of Irs1 and Irs2 expression. We intercrossed $Irs1^{L/L}$ mice and $Irs2^{L/L}$ mice with muscle creatine kinase (MCK)-Cre transgenic mice to produce mice without muscle Irs1 (MKO1 mice), Irs2 (MKO2 mice), or either of the Irs proteins (MDKO mice) (8, 13, 38). The *MCK-Cre* transgene is expressed in striated muscle and in cardiac myocytes, so both tissues are expected to be affected (35). At 2 weeks of age, immunoblotting revealed a striking reduction of Irs1 protein in skeletal muscle extracts from MKO1 and MDKO mice and Irs2 protein in muscle extracts of MKO2 and MDKO mice (Fig. 1A to C). Skeletal muscle extracts contained some residual Irs1 or Irs2 protein, which could be attributed to the incomplete deletion of the floxed alleles in a small fraction of myofibers or to the presence of other cell types in the tissue, including fibroblasts, adipocytes, peripheral nerves, endothelial cells, Schwann cells, or satellite cells (8).

The MKO1 and MKO2 mice showed no perinatal lethality and survived until the experiment was terminated at 2 years of age; however, MDKO mice died suddenly between 2 to 3 weeks of age (Fig. 1D). Morphological examination of the liver, brain, and adipose tissues revealed no detectable abnormalities in MDKO mice that could explain their premature death, and necropsy confirmed that MDKO mice fed normally until death (Table 1). Irs protein concentrations in MDKO liver, adipose, and brain tissues were normal (data not shown). In contrast, at 2 weeks of age, the hearts of MDKO mice were slightly smaller, though statistically indistinguishable, than

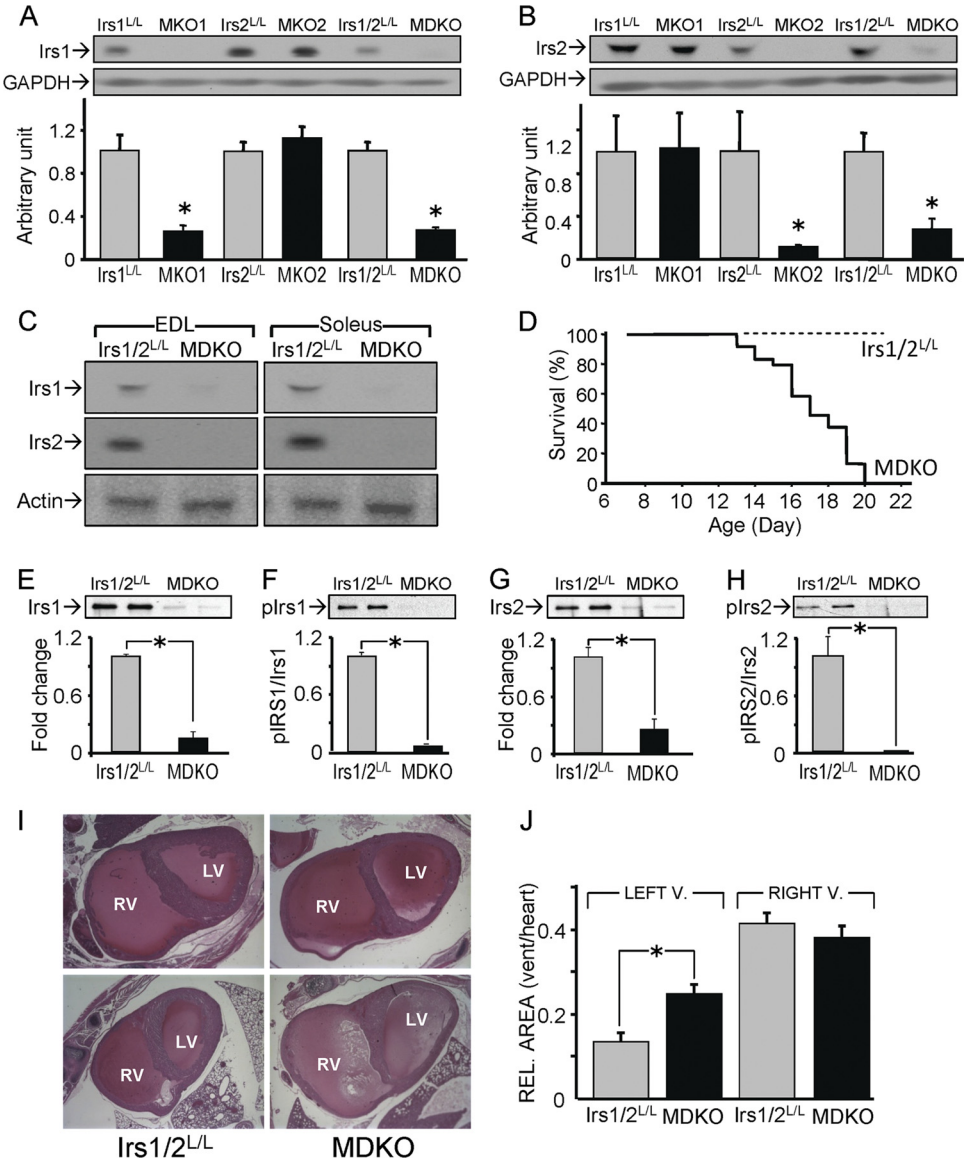

FIG. 1. Irs1 and Irs2 in skeletal and cardiac muscle. (A and B) Protein content of Irs1 (A) and Irs2 (B) analyzed by specific immunoblotting of gastrocnemius muscle lysates from 2-week-old mice of the indicated genotype ($n = 6$; $*$, $P < 0.05$). Error bars represent standard error of the mean (SEM). (C) Representative immunoblot of IRS1 and IRS2 proteins in EDL and soleus muscles of control ($Irs1/2^{L/L}$) and MDKO mice. (D) Survival curve of MDKO mice and $Irs1/2^{L/L}$ mice. (E to H) Protein concentration and tyrosine phosphorylation of Irs1 and Irs2 in cardiac muscle extracts from 2-week-old control and MDKO mice ($n = 2$; $*$, $P < 0.05$). (I) Transverse sections of cardiac muscle from two $Irs1/2^{L/L}$ and two MDKO mice at 2 weeks of age. RV, right ventricle; LV, left ventricle. (J). Relative sizes of the left and right ventricles (ventricle area/heart area) from $Irs1/2^{L/L}$ and MDKO mice ($n = 4$; $*$, $P < 0.05$).

those of the controls (CNTR) (CNTR, 41.9 ± 1.1 mg; MDKO, 37.8 ± 2.7 mg) ($P = 0.171$, $n = 6$) and the ratios of heart to body weight were equal (CNTR, 5.9 ± 0.4; MDKO, 6.0 ± 1.4) ($n = 6$) (Table 1). Regardless, Irs1 and Irs2 in MDKO cardiac muscle extracts were barely detected, and tyrosine phosphorylation of Irs1 and Irs2 was entirely absent (Fig. 1E to H). Compared to control hearts, transverse sections of the MDKO hearts revealed significantly dilated left ventricles, consistent with the progression of dilated cardiomyopathy (Fig. 1I and J). Because similar pathologies (and time courses of lethality) have been observed in mice deficient in muscle Ir and Igf1r (35), as well as in mice lacking Irs1 and Irs2 specifically in cardiac muscle (49), we conclude provisionally that the sudden death of MDKO mice was caused by cardiomyopathy. Whereas the role of Irs1 and Irs2 in cardiomyocytes is under investigation elsewhere (49), in this report, we focus upon signaling and metabolism in the skeletal muscle of 2-week-old mice.

Deficiency of both Irs1 and Irs2 impairs skeletal muscle growth. There was a mild yet statistically significant reduction in the body mass and body length of MDKO mice compared to those of control mice at 2 weeks of age (Table 1). Growth retardation of lean body mass could account for the 13% body weight reduction (Table 1). Bone mineral densities in MDKO

TABLE 1. Body composition and tissue-to-body weight ratios of control and muscle-specific Irs1 and/or Irs2 knockout mice

Characteristic[a]	Value for indicated mice[b]					
	Control MKO1	MKO1	Control MKO2	MKO2	Control MDKO	MDKO
Body weight (g)	8.2 ± 0.5	8.1 ± 0.4	8.7 ± 0.2	8.4 ± 0.6	7.4 ± 0.2	6.4 ± 0.3*[c]
Body length (cm)	6.6 ± 0.1	6.5 ± 0.1	6.6 ± 0.1	6.4 ± 0.2	6.3 ± 0.1	5.7 ± 0.2*
BMD (mg/cm^2)	0.025 ± 0.001	0.025 ± 0.001	0.025 ± 0.001	0.025 ± 0.001	0.024 ± 0.001	0.024 ± 0.001
Lean mass (g)	6.4 ± 0.4	6.3 ± 0.3	6.9 ± 0.2	6.5 ± 0.4	6.0 ± 0.2	5.2 ± 0.2*
Fat mass (g)	1.7 ± 0.2	1.6 ± 0.2	1.7 ± 0.1	1.7 ± 0.1	1.5 ± 0.0	1.5 ± 0.1
Fat/body (%)	20.1 ± 1.1	20.3 ± 1.6	20.4 ± 0.6	20.0 ± 0.5	20.3 ± 0.6	22.4 ± 0.6*
Heart/body (%)	5.9 ± 0.2	5.7 ± 0.1	6.4 ± 0.3	6.2 ± 0.3	5.9 ± 0.2	6.0 ± 0.6
Liver/body (%)	37.2 ± 1.8	39.4 ± 0.7	34.5 ± 0.8	32.3 ± 0.7	35.4 ± 1.2	34.2 ± 0.9
BAT/body (%)	6.6 ± 0.6	6.8 ± 0.8	5.6 ± 0.3	5.0 ± 0.3	6.0 ± 0.5	6.6 ± 0.3
WAT/body (%)	6.8 ± 1.0	7.4 ± 0.9	6.3 ± 0.9	5.9 ± 1.1	3.8 ± 0.5	4.2 ± 0.8
Pancreas/body (%)	7.7 ± 0.2	8.8 ± 0.6	6.5 ± 0.3	5.7 ± 0.5	6.3 ± 0.5	6.7 ± 0.9
Kidney/body (%)	14.7 ± 0.4	16.2 ± 0.4	13.3 ± 0.6	13.2 ± 0.4	15.6 ± 0.6	16.3 ± 0.6
Spleen/body (%)	5.4 ± 0.6	6.0 ± 0.4	5.2 ± 0.4	5.2 ± 0.4	4.6 ± 0.3	5.4 ± 0.3
Lung/body (%)	10.4 ± 0.4	10.6 ± 0.4	10.3 ± 0.4	10.4 ± 0.6	11.6 ± 0.3	12.4 ± 0.6

[a] BMD, bone mass density; BAT, brown adipose tissue; WAT, white adipose tissue.
[b] Tissues were dissected from the indicated mice ($n = 6$), and wet weight (± standard error) was measured.
[c] *, $P < 0.05$.

mice were equal to those in the corresponding control mice, and there were no significant changes in the masses of other tissues or organs in MDKO mice (Table 1). Given that skeletal muscle comprises much of whole-body lean mass, we examined the contribution of Irs1 and Irs2 to skeletal muscle growth. The skeletal muscle mass of MKO1 or MKO2 mice was largely normal in comparison to that of age-matched control mice; however, a mild yet significant reduction of tibialis anterior (TA) muscle mass in the MKO1 mice was observed (Fig. 2A). Compared to controls, the average ratio of muscle to body weight was reduced significantly in MDKO gastrocnemius (37%; $P < 0.001$), MDKO tibialis anterior (30%; $P < 0.001$), and MDKO quadriceps (40%; $P < 0.001$) (Fig. 2A). Moreover, gastrocnemius muscle protein content in MKO1 and MDKO mice was significantly decreased (14% and 37%, respectively) (Fig. 2B). This decrease in protein content (37%) equaled the overall reduction of skeletal muscle mass (37%) in the MDKO mice, suggesting that the loss of protein accounts for the total muscle mass reduction. Morphological examination revealed that the TA muscle cross section of MDKO mice was reduced 38% compared to that of the control mice (Fig. 2C). The individual myofiber cross-sectional area was also reduced, as revealed by the skewed myofiber size distribution (CNTR median size, 95% confidence interval [CI] of 378 to 421; MDKO median size, 95% CI of 229 to 252) (Fig. 2D and E). Taken together, these data suggest that growth retardation of MDKO mice was restricted largely to skeletal muscle and that Irs1 appears to contribute more to muscle growth than Irs2.

Insulin-like signaling is impaired in MDKO skeletal muscle. We investigated the effect of Irs1 and/or Irs2 deficiency on insulin signal transduction in gastrocnemius muscle. Two-week-old mice were treated for 5 min with insulin (vena cava injection), followed by removal of the muscle tissue. Compared to MKO1, MKO2, or control tissue, insulin-stimulated Akt phosphorylation ($T308^{Akt}$) was barely detected in MDKO muscle extracts by immunoblotting (Fig. 3A to C). By comparison, an insignificant ($P = 0.26$) reduction of $T308^{Akt}$ phosphorylation was observed in MKO1 mice (Fig. 3A), and no reduction was observed in MKO2 mice (Fig. 3B). Insulin-induced phosphorylation of $S473^{Akt}$ was reduced significantly (50%) in MKO1 and MDKO mice (Fig. 3D and F), whereas $S473^{Akt}$ phosphorylation was not reduced in the MKO2 mice (Fig. 3E). Therefore, Irs1 has a significant role in the activation of $T308^{Akt}$ phosphorylation in skeletal muscle during insulin stimulation; however, a role for Irs2 may be observed in the absence of Irs1.

Isolated skeletal muscles from control and MDKO mice were incubated with IGF1 to evaluate the role of Irs1 and Irs2 in the transmission of the skeletal muscle hypertrophic signal (5, 19). Compared to control muscle samples, the IGF1-stimulated phosphorylation of $T308^{Akt}$ was impaired in skeletal muscle from MDKO mice (Fig. 3G). Consistent with these results, IGF1-mediated activation of the mTOR pathway, including the phosphorylation of TCS2 ($T1462^{TSC2}$), S6K ($T389^{S6K}$), ribosomal protein S6 ($S240^{S6}$ $S244^{S6}$), and 4EBP1 ($T37^{4EBP1}$), was also significantly reduced in the skeletal muscle of MDKO mice (Fig. 3H to K).

The skeletal muscle atrogene program is upregulated in MDKO mice. Insulin-like signals are critical suppressors of the skeletal muscle atrophy gene program, in part via inhibition of Foxo transcription factors (5, 19). Akt-mediated phosphorylation of Foxo1/3 reduces their nuclear localization and inhibits their transcriptional effects (46). In skeletal muscles from MDKO mice, the phosphorylation of Foxo1 (S256) and Foxo3 (S253) was reduced significantly, by about 50%, whereas the slight reduction in MKO1 or MKO2 muscle did not reach significance (Fig. 4A and B). Consistent with increased concentrations of unphosphorylated Foxo1/3 in the skeletal muscle of MDKO mice, expression of genes involved in skeletal muscle atrophy increased significantly, including MuRF1 (muscle-specific RING finger protein 1), Becn1 (autophagy-related gene [Atg] 6 or Beclin1), Lamp2a (lysosomal-associated membrane protein 2), cathepsin, LC3 (microtubule-associated protein 1 light chain 3α), Gabarapl1 [GABA(A) receptor-associated protein-like 1], and atrogin (F-box only protein 32); however, the housekeeping gene Gapdh remained

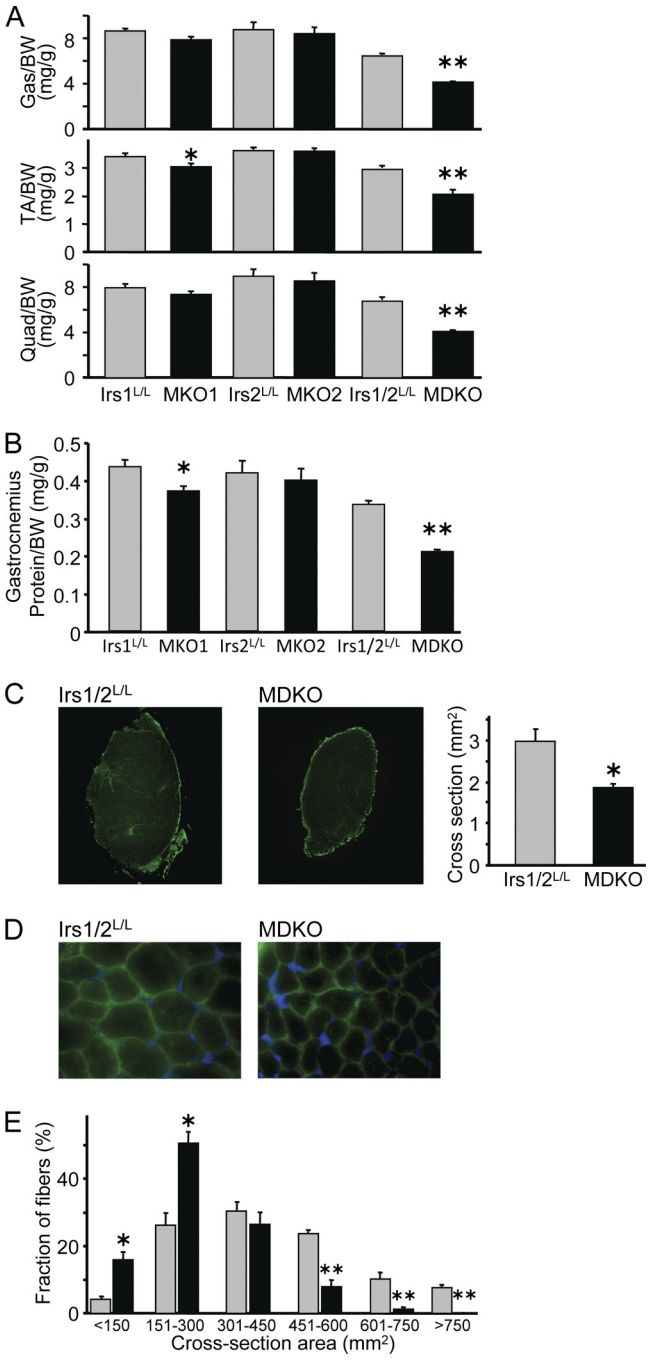

FIG. 2. Skeletal muscle protein content and cross-sectional area. (A) Relative average weight (mg/g body weight [BW]) of gastrocnemius (Gas), tibialis anterior (TA), and quadriceps (Quad) muscle in 2-week-old male mice ($n = 6$; *, $P < 0.05$; **, $P < 0.005$). (B) Relative protein content (mg/g body weight) in gastrocnemius isolated from 2-week-old male mice. (C) Representative cross sections of tibialis anterior (TA) muscle of control and MDKO mice stained with dystrophin; cross-sectional area of TA muscle ($n = 6$; *, $P < 0.05$). (D, E) Representative cross sections of TA muscle of control and MDKO mice (D) stained with dystrophin and DAPI (4′,6-diamidino-2-phenylindole) to determine the distribution of the myofiber cross-sectional area (E) in 2-week-old male mice ($n = 6$; *, $P < 0.05$; **, $P < 0.005$).

unchanged (Fig. 4C). The genes involved in skeletal muscle atrophy are known to be direct targets of the Foxo transcription factors (60). This transcriptional reprogramming of MDKO skeletal muscle was expected to increase the rate of proteolysis (60) Consistent with this, there was an increase in amino acid release from isolated fast-twitch/glycolytic EDL and slow-twitch/oxidative soleus muscles of MDKO mice (Fig. 5A), and the protein content of both muscle types was consistently reduced (Fig. 5B).

Metabolism of glucose to lactate in MDKO skeletal muscle. Because skeletal muscle is a major site of insulin-stimulated glucose disposal, we investigated whether the genetic ablation of skeletal muscle Irs1 and/or Irs2 dysregulated nutrient homeostasis. During random feeding, the MDKO mice displayed mildly depressed blood glucose with markedly elevated blood lactate concentration, whereas the MKO1 and MKO2 mice were normal (Fig. 5C and D). Fasting blood glucose levels in control and MDKO mice were equal, but fasting blood lactate in MDKO mice was elevated by about 2-fold (Fig. 5E and F, time = 0 min). These results suggested an altered metabolic fate of glucose in the MDKO mice, owing apparently to an increased conversion of glucose to lactate in skeletal muscle.

To establish whether lactate production in the MDKO mice depended upon the circulating glucose concentration *per se*, we altered the glucose availability to skeletal muscle *in situ* by injecting glucose or insulin into control and MDKO mice. Under the challenge of a glucose load, MDKO mice and control mice displayed identical glucose tolerances (Fig. 5E). Following the glucose injection, blood lactate increased with similar time courses by about 30% in the control and MDKO mice, but the absolute concentration of lactate was always significantly higher in the MDKO mice (Fig. 5F). Like the glucose concentration, lactate returned to the basal concentration 2 h after the glucose injection, consistent with the hypothesis that excess circulating glucose was converted to lactate.

During the insulin tolerance test, MDKO mice displayed only mild insulin resistance compared to that displayed by the control mice (Fig. 5G). Given the lack of insulin-stimulated glucose uptake into isolated MDKO muscle seen in separate experiments (Fig. 6D and see below), this may have owed partly to the disappearance of glucose into nonmuscle tissues. Consistent with the hypothesis that circulating glucose is rapidly converted into lactate in MDKO mice, the decrease in blood glucose concentration in insulin-injected MDKO mice was paralleled by a decrease in blood lactate (Fig. 5H). In comparison, the blood lactate concentration was low and unchanged following insulin injection of control mice (Fig. 5H).

AMPK is activated in skeletal muscle of MDKO mice. The conversion of circulating glucose to lactate in MDKO skeletal muscle suggested decreased oxidation of glucose via the tricarboxylic acid (TCA) cycle that could, in turn, lead to energy depletion and an increase in the cellular AMP/ATP ratio (39, 60). Consistent with this, the rate of glucose oxidation was significantly decreased in both EDL and soleus muscles from MDKO mice (Fig. 6A) in conjunction with increased expression of Pdk4, which regulates the entry of pyruvate from glycolysis into the TCA cycle (Fig. 6E). The ATP concentration in MDKO skeletal muscle decreased significantly (CNTR, 353 ± 24 μmol/g; MDKO, 269 ± 24 μmol/g) ($P = 0.04$), while the AMP concentration increased (CNTR, 4.6 ± 0.8 μmol/g;

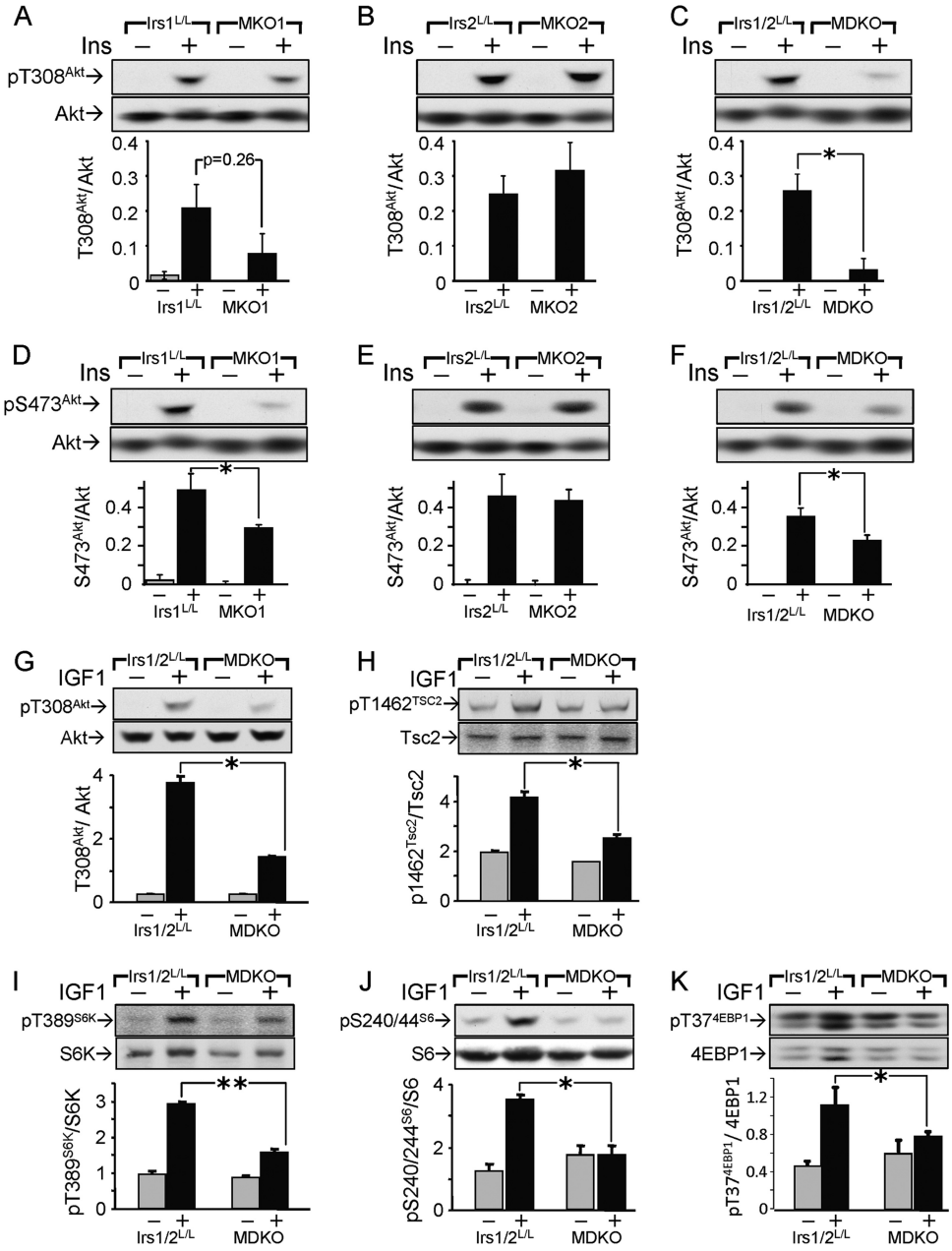

FIG. 3. The effect of skeletal muscle deficiency of Irs1 and Irs2 upon signaling. (A to F) MKO1, MKO2, or MDKO mice were treated with saline or insulin (Ins) for 5 min, followed by an immunoblot assay of Akt phosphorylation in gastrocnemius muscle with phosphospecific antibodies against Thr308 (A to C) or Ser473 (D to F). (G to K) EDL muscles isolated from control or MDKO mice were treated without or with IGF1 for 30 min; tissue extracts were analyzed by immunoblotting with phospho-specific and non-phospho-specific antibodies against Akt, Tsc2, S6k, S6, or 4EBP1. Error bars represent SEM ($n = 4$; $*$, $P < 0.05$; $**$, $P < 0.01$).

MDKO, 10.1 ± 1.4 μmol/g) ($P = 0.01$). In combination, these changes gave rise to a 3-fold increase in the AMP/ATP ratio in MDKO skeletal muscle compared to that in control muscle (Fig. 6B). Consistent with these data, AMPK phosphorylation was increased significantly in MDKO skeletal muscle, with smaller effects detected in MKO1 and MKO2 mice (Fig. 6C). Compared to muscle from control mice, the phosphorylation of ACC (acetyl-CoA carboxylase)—a direct target of AMPK—was strongly increased in MDKO muscle, and smaller increases were noted in MKO1 and MKO2 muscle (Fig. 6C). Thus, normal signaling by both Irs1 and Irs2 appears to be required for normal glucose metabolism and ATP production to attenuate the activation of the AMP/ATP→AMPK→ACC signaling cascade.

AMPK suppresses cell growth and biosynthetic processes in part through its inhibition of the rapamycin-sensitive mTOR (mTORC1) pathway. AMPK phosphorylation of the TSC2 tumor suppressor and the mTORC1 binding partner Raptor contribute to this inhibition (23). Compared to the control, Raptor was strongly phosphorylated in MDKO muscle on the

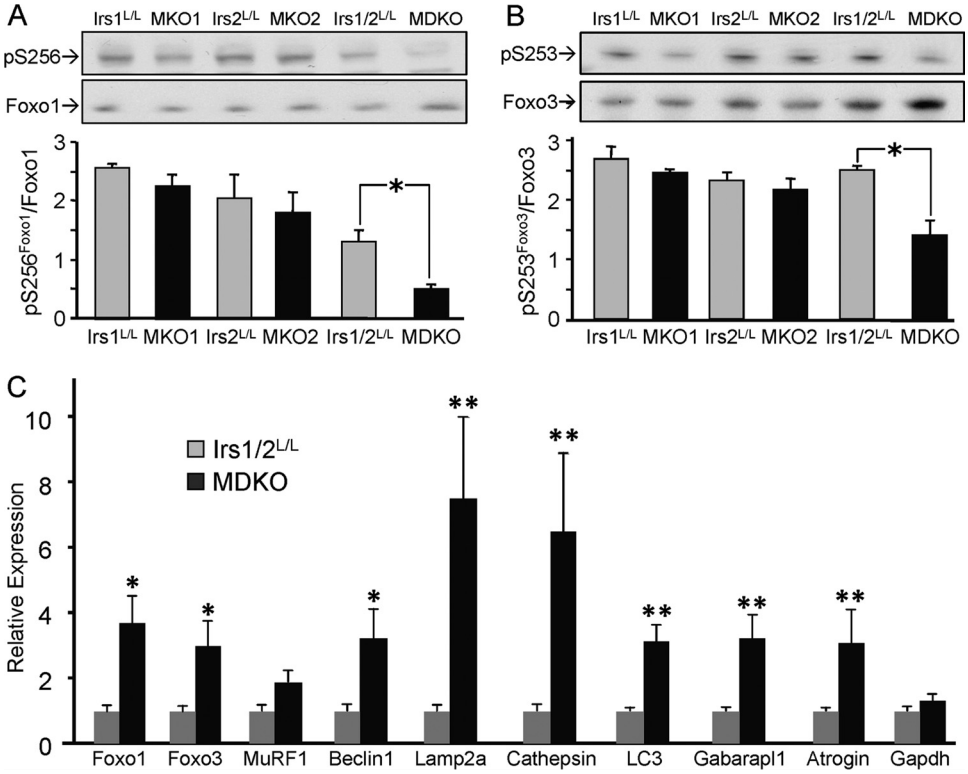

FIG. 4. FoxO signaling and gene expression in skeletal muscle. (A and B) Skeletal muscle Foxo1 (A) or Foxo3 (B) phosphorylation in gastrocnemius muscle lysates from control, MKO1, MKO2, or MDKO mice. Muscles were isolated from 2-week-old male mice and analyzed by immunoblotting with phospho-specific or protein-specific antibodies. The mean quantified signals are compared; error bars represent SEM ($n = 6$; *, $P < 0.05$). (C) Relative mRNA concentrations of genes involved in skeletal muscle atrophy in 2-week-old Irs1/2$^{L/L}$ or MDKO mice were determined by real-time PCR ($n = 6$; *, $P < 0.05$; **, $P < 0.005$).

highly conserved AMPK site (S792^{Raptor}) (Fig. 6C). In contrast, the phosphorylation of TSC2 on a conserved AKT site (S1462^{TSC2}) was decreased in MDKO muscle (Fig. 6C), consistent with reduced insulin-like signaling (26). Similar effects were difficult to detect in the MKO1 and MKO2 muscle. Together, these results demonstrate the inhibition of mTOR-mediated muscle growth in the MDKO mice.

Given the potential for activated AMPK signaling to affect muscle glucose disposal (15, 58), we measured glucose uptake into isolated skeletal muscle with or without insulin stimulation; importantly, the preincubation/equilibration of skeletal muscles in this *in vitro* metabolic assay diminishes the potential contribution of altered nutrient, hormonal, or other systemic factors in the MDKO mice. Both EDL and soleus muscles from control mice displayed normal insulin-stimulated glucose uptake during *in vitro* incubation; however, the effect of insulin upon glucose uptake into muscle from MDKO mice was insignificant (Fig. 6D). In contrast, basal glucose uptake in MDKO muscle was substantially elevated in conjunction with increased AMPK activation, reaching the same levels as those of the insulin-stimulated glucose uptake seen in control muscle (Fig. 6D). This increase in basal glucose uptake was not the result of altered glucose transporter expression, as the concentrations of the GLUT1 and GLUT4 transporter proteins were significantly reduced in MDKO muscle lysates (Fig. 6F and G). Increased basal glucose uptake—but impaired glucose oxidation—was compatible with the increased AMP/ATP ratio of isolated MDKO muscles (Fig. 6B) and accompanied by increased lactate release (Fig. 6H), mirroring the *in vivo* hyperlactatemia of MDKO mice. In comparison with control muscle, the glycogen content in MDKO muscle was reduced significantly (Fig. 6I). Consistent with the activation of AMPK→ACC signaling, both EDL and soleus muscles from MDKO mice displayed increased palmitate oxidation under *in vitro* incubation conditions (Fig. 6J).

DISCUSSION

Insulin-like signaling in skeletal muscle is initiated by the activation of the insulin and IGF1 receptor tyrosine kinases (35), which are linked to downstream pathways through the Irs1 and Irs2 branches of the cascade. Based upon our analyses of insulin- and IGF1-stimulated Akt→mTORC1 signaling, Irs1 has a slightly greater, albeit not exclusive, role in insulin-like signaling in muscle than Irs2. Consistent with this, MKO1 mice display a small reduction in muscle mass and protein content, whereas no reduction in MKO2 mice is detected. These results are consistent with previous work showing that conventional systemic *Irs1* knockout mice are smaller than control mice (2, 57). Regardless, when the Irs1 branch is inactivated in MKO1 muscle, Irs2 can promote Akt→mTORC1 signaling and muscle growth. Since the deletion of both Irs1 and Irs2 further reduces muscle growth in MDKO mice—and either Irs1 or Irs2 can prevent sudden death—we conclude that both Irs proteins

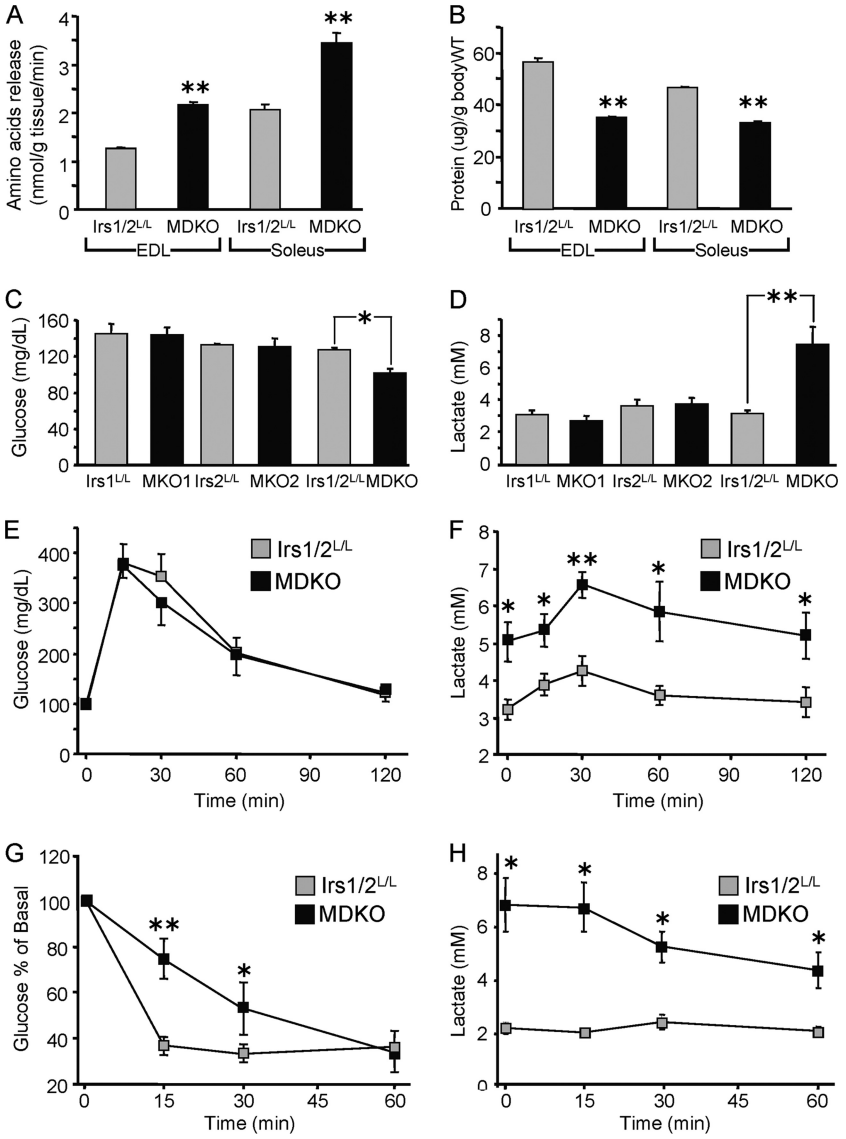

FIG. 5. Metabolic homeostasis in MDKO mice. (A) The rate of amino acid release from EDL or soleus muscles of 2-week-old Irs1/2$^{L/L}$ or MDKO mice ($n = 5$ or 6; **, $P < 0.05$). (B) Protein content of EDL and soleus muscles of Irs1/2$^{L/L}$ or MDKO mice ($n = 5$ or 6; **, $P < 0.05$). (C and D) Blood glucose and lactate concentrations in 2-week-old Irs1/2$^{L/L}$ or MDKO mice ($n = 6$; *, $P < 0.05$; **, $P < 0.005$) sampled in the morning during random feeding. Error bars represent SEM. (E and F) Lactate and blood glucose concentrations in fasted 2-week-old Irs1/2$^{L/L}$ or MDKO mice after a morning bolus glucose injection ($n = 9$ or 10; *, $P < 0.05$; **, $P < 0.005$). Error bars represent SEM. (G and H) Blood glucose and lactate concentrations in 2-week-old Irs1/2$^{L/L}$ or MDKO mice fasted 4 h before injection with insulin ($n = 6$ or 7; *, $P < 0.05$; **, $P < 0.005$). Error bars represent SEM.

contribute to insulin-like signaling in skeletal and cardiac muscles.

Insulin-like signals promote muscle growth through the Akt→mTOR pathway (5, 19). Compared to control mice, Akt phosphorylation at T308^{AKT} and S473^{AKT} in MKO1 muscle is mildly impaired, whereas Akt phosphorylation in MKO2 mice is normal. Moreover, insulin-stimulated phosphorylation of T308^{AKT} and S473^{AKT} in MDKO muscle is lower but is statistically indistinguishable from MKO1 muscle. These results support the conclusion that Irs1 has a greater role in the phosphorylation/activation of Akt in skeletal muscle than Irs2. Upon deletion of Irs1—or both Irs1 and Irs2—insulin-stimulated T308^{AKT} phosphorylation is more strongly reduced than S473^{AKT} phosphorylation. This difference might arise because T308^{AKT} is a direct target of PDK1, which is immediately downstream of phosphatidylinositol (PI) 3-kinase, whereas S473^{AKT} phosphorylation is off this pathway and mediated at least in part by mTORC2 (33). The role of mTORC2 in skeletal muscle S473^{AKT} phosphorylation in mice is confirmed by muscle-specific deletion of Rictor, a component of the mTORC2 complex (7, 32). The mechanism of mTORC2 activation in response to insulin is unknown and might involve a pathway distinct from that of Irs1 and Irs2.

Skeletal muscle proteolysis is an important source of amino acids during fasting, and Foxo transcription factors promote the expression of critical proteins that mediate this process (28,

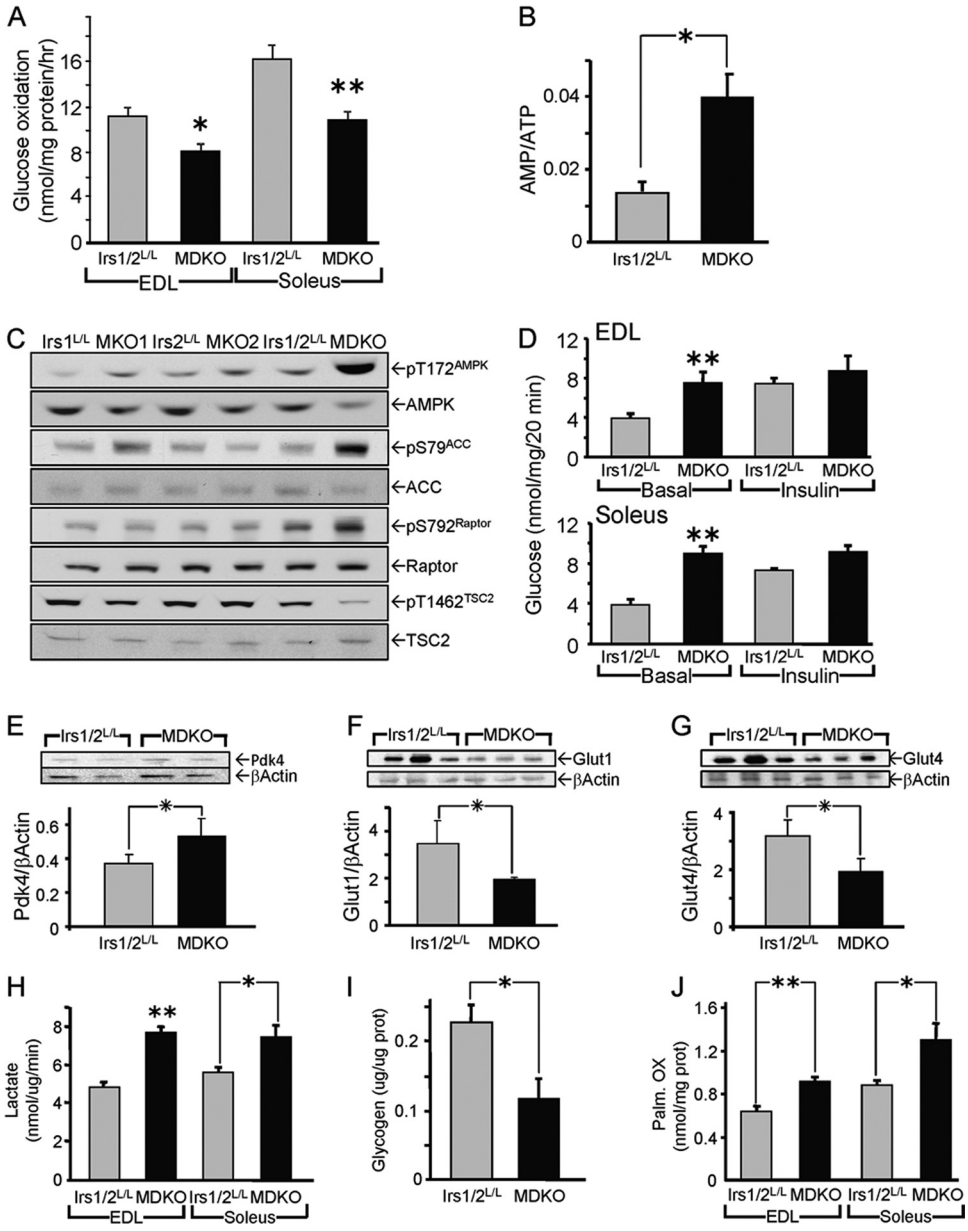

FIG. 6. Activation of the AMPK pathway and altered metabolism in skeletal muscle from MDKO mice. (A) Rate of glucose oxidation in isolated EDL and soleus muscles from Irs1/2$^{L/L}$ or MDKO mice ($n = 5$ or 6; *, $P < 0.05$; **, $P < 0.01$) (B) AMP/ATP ratio in Irs1/2$^{L/L}$ or MDKO muscle (gastrocnemius) ($n = 5$ or 6; *, $P < 0.05$). (C) Expression and phosphorylation, analyzed by immunoblotting, of AMPK, ACC, Raptor, and Tsc2 in gastrocnemius muscle lysates from 2-week-old control, MKO1, MKO2, or MDKO mice ($n = 6$). (D) Rate of glucose uptake in isolated EDL and soleus muscles from Irs1/2$^{L/L}$ or MDKO mice without or with insulin stimulation ($n = 5$ or 6; **, $P < 0.01$). Error bars represent SEM. (E to G) Protein contents of PDK4, GLUT1, and GLUT4 in gastrocnemius muscles from Irs1/2$^{L/L}$ or MDKO mice ($n = 5$ or 6, *, $P < 0.05$) (H) Rate of lactate release from isolated EDL and soleus muscles from Irs1/2$^{L/L}$ or MDKO mice ($n = 5$ or 6; *, $P < 0.05$; **, $P < 0.01$). (I) Gastrocnemius muscle glycogen content in Irs1/2$^{L/L}$ or MDKO mice ($n = 8$; *, $P < 0.05$). (J) Rate of palmitate oxidation (Palm. OX) in EDL and soleus muscles from Irs1/2$^{L/L}$ or MDKO mice ($n = 5$ or 6; *, $P < 0.05$; **, $P < 0.01$). Error bars represent SEM.

50, 52, 54, 60). Overexpression of Foxo1/3 is sufficient to activate proteasomal and autophagy/lysosomal degradation of skeletal muscle protein (28, 40, 60). Foxo1/3 activity also promotes atrophy during muscle disuse and renal failure (41, 61). Our results show that Irs1 and Irs2 signaling is required to suppress this catabolic pathway even when nutrients are abundant, at least in part by promoting Akt-mediated phosphorylation of Foxo1 and Foxo3, which inhibits their transcriptional activities. The deletion of Irs1 or Irs2 alone has mild and insignificant effects upon Foxo1 and Foxo3 phosphorylation, suggesting that either Irs protein can regulate skeletal muscle Foxo1/3; however, deletion of both Irs1 and Irs2 in the MDKO mice reduces significantly, albeit incompletely, the phosphorylation of Foxo1/3 (S256^{Foxo1} and S253^{Foxo3}).

In the absence of Irs1 alone (MKO1 muscle), insulin-stimulated Akt phosphorylation is reduced, but Foxo1/3 phosphor-

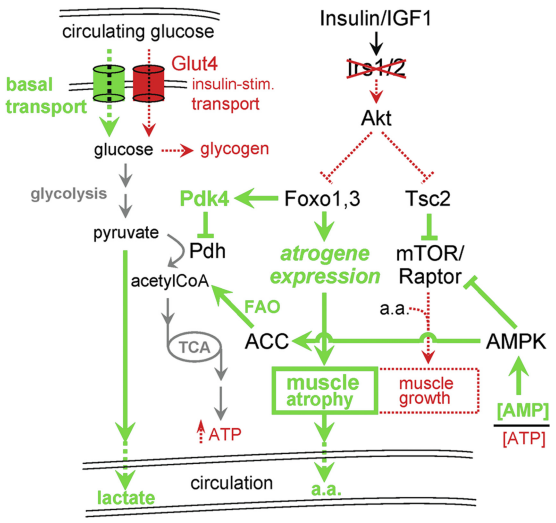

FIG. 7. Model of Irs-dependent regulation of skeletal muscle growth and metabolism. Arrows indicate upregulation/activation, and blunt ends indicate downregulation/repression in normal tissue. Those pathways enhanced in MDKO muscle are presented as boldfaced green lines/type and those diminished are presented as thin and dashed red lines/red type. Pathways/intermediate steps not directly assayed are shown as solid gray lines/type. Proteins are capitalized, and the upregulation of transcription is shown in italics. ETC, mitochondrial electron transport chain; FAO, fatty acid oxidation; a.a., amino acids; Pdh, pyruvate dehydrogenase.

ylation remains unaltered, suggesting that the residual level of Akt activity is sufficient to regulate Foxo1/3. However, Foxo activity is also regulated by AMPK (21), which is strongly activated in MDKO but not MKO1 muscle. Thus, a combination of decreased Akt activation and increased AMPK signaling may account for the decrease in Foxo1/3 phosphorylation specifically in MDKO muscle. Regardless, the diminished Foxo1/3 phosphorylation is associated with increased expression of Foxo-regulated proteasomal and autophagy genes (atrogenes) that promote protein degradation (28, 40, 60) and amino acid efflux from MDKO muscle (Fig. 7). Impaired mTORC1 pathway signaling in the absence of Irs1/2 may further contribute to the reduced mass and protein content of MDKO muscle via dysregulation of muscle protein synthesis at the level of the translational machinery (5, 19). Additionally, mTORC1 signaling has been shown to contribute to the regulation of genes involved in atrophy, including MuRF1 and atrogin1 (34, 51). Thus, signals transduced by Irs1 and Irs2 together are essential to suppress skeletal muscle proteolysis during nutrient abundance and promote the mTORC1-mediated muscle growth/hypertrophic signal (Fig. 7).

Insulin signaling regulates the energy balance in skeletal muscle by stimulating glucose uptake and glycogen storage (53). Previous studies that utilized systemic knockout mouse models of Irs1 or Irs2 demonstrated that neither Irs1 nor Irs2 is essential for insulin-induced skeletal muscle glucose uptake (18, 24, 25). In contrast, we provide evidence that ablation of both Irs1 and Irs2 abolishes insulin-stimulated glucose uptake in skeletal muscle; therefore, both Irs proteins are critical, and have overlapping roles, in mediating the effect of insulin. Akt has been recognized as a critical regulator of both skeletal muscle glucose transport (10, 17, 43) and activation of glycogen synthesis (12, 56). Consistent with the impaired Akt activation in MDKO skeletal muscle, glycogen stores are significantly decreased, further supporting that the Irs1/2 proteins are required to maintain the skeletal muscle energy balance.

Glucose transport into skeletal muscle is essential for nutrient homeostasis, as the deletion of the insulin-regulated Glut4 transporter (solute carrier family 2, member 4) in muscle promotes insulin resistance and glucose intolerance (62). Thus, skeletal muscle insulin resistance was thought originally to be a prominent cause of hyperglycemia that could progress to diabetes; however, this hypothesis is not supported by the deletion of insulin and IGF1 receptors or by the deletion of Irs1 and Irs2 from skeletal muscle (35, 37). Compared to control mice, our MDKO mice display mild hypoglycemia rather than elevated circulating glucose. Moreover, MDKO mice display normal glucose tolerance, in comparison with that displayed by control mice, during an intraperitoneal glucose challenge. Similar results were observed with mice lacking skeletal and cardiac muscle insulin and IGF1 receptors (35). These results are unexpected because insulin-stimulated glucose influx into skeletal muscle is thought to be critical for glucose homeostasis (53). Although insulin-stimulated glucose uptake into MDKO muscle is lost, basal glucose influx increases to the level ordinarily measured during insulin stimulation. Thus, in contrast with the impaired insulin sensitivity of type 2 diabetes, the nearly complete skeletal muscle insulin resistance in MDKO mice does not give rise to glucose intolerance or hyperglycemia.

Glucose metabolism is nevertheless significantly dysregulated in MDKO muscle. Ordinarily, glucose is transported into myocytes via Glut4, where it is phosphorylated by hexokinase and utilized in the glycolytic/oxidative phosphorylation pathway to generate ATP or incorporated into glycogen by glycogen synthase (53). However, compared to control mice, ATP and glycogen concentrations are reduced in MDKO muscle, and lactate production is increased under both fasting and postprandial conditions. Since glucose influx into MDKO muscle is constitutively elevated, the blood lactate concentration fluctuates in parallel with the blood glucose concentration. This metabolism of glucose to lactate—or "carbon intolerance" of the skeletal muscle—provides an alternative route of glucose disposal that contributes to the maintenance of normoglycemia in MDKO mice (Fig. 7).

Among insulin-independent pathways, AMPK is one of the most prominent candidates in the activation of skeletal muscle glucose uptake (15, 58). AMPK serves as an energy sensor to detect an increase in the AMP/ATP ratio and, in turn, restores energy balance by suppressing anabolic pathways that consume energy while promoting catabolic pathways, including fatty acid oxidation, that mobilize or generate energy (27, 39). Consistent with reduced glycogen storage and an increased AMP/ATP ratio, AMPK is strongly activated in MDKO skeletal muscle, where it promotes phosphorylation of ACC and Raptor to increase fatty acid oxidation and further decrease protein synthesis, respectively (Fig. 7) (23, 59). Thus, Irs1 and Irs2 signaling is actively required to suppress skeletal muscle fasting/catabolic pathways, even in the presence of adequate nutrition, through maintenance of an AMP/ATP ratio sufficient to suppress AMPK activation.

Treatment of isolated mouse skeletal muscle with AICAR (a pharmacological activator of AMPK) increases GLUT4 translocation (15, 58) and skeletal muscle glucose uptake concomitant with an increase in lactate release from the tissue due to increased glycolysis (44). Consistent with this, the derepressed skeletal muscle AMPK pathway of MDKO mice increases glucose uptake under basal conditions, associated with mild hypoglycemia and increased lactate release from the muscles (Fig. 7). Importantly, as both GLUT1 and GLUT4 protein content in MDKO muscles is decreased, the observed increase in basal glucose uptake likely owes to the effects of activated AMPK signaling upon glucose transporters (1, 4) rather than increased transporter protein expression. In contrast, the impaired insulin-induced glucose uptake seen in MDKO muscle is consistent with the observed decrease in GLUT4, which is critical for insulin-mediated skeletal muscle glucose uptake (62).

The flexibility of skeletal muscle to switch substrate utilization is central for energy homeostasis (14). Under postprandial conditions, insulin stimulates skeletal muscle glucose uptake and utilization. During fasting, when circulating glucose concentrations fall and fatty acid concentrations rise, fatty acid oxidation by skeletal muscle increases (14, 30). Although substrate availability is postulated to be the major factor in the regulation of the metabolic flexibility of skeletal muscle, Foxo1 also controls this switch by upregulating three key enzymes: Pdk4 (pyruvate dehydrogenase kinase 4), which inhibits Pdh (pyruvate dehydrogenase); lipoprotein lipase (LPL), which hydrolyzes plasma triglycerides into fatty acids; and CD36 (fatty acid translocase), which facilitates fatty acid uptake into skeletal muscle (6, 14, 16, 30). Notably, inhibition of Pdh activity by Pdk4 reduces the conversion of glycolytically derived pyruvate into acetyl-CoA, thereby diverting glucose flux to lactate and away from oxidation in the TCA cycle (6, 16). Consistent with this, glucose oxidation in MDKO skeletal muscles is decreased, concomitant with increased expression of PDK4 (Fig. 7).

The switch from glucose oxidation to lactate production might contribute directly to the observed decrease in the ATP concentration in MDKO skeletal muscle; however, the resultant AMPK-mediated upregulation of fatty acid oxidation fails to completely restore the energy balance. Several mechanisms may contribute to this state. First, degradation of cellular proteins is an energy-consuming process. ATP is required for the activation of ubiquitin by a ubiquitin-activating enzyme (E1) as well as the engagement, unfolding, and translocation of polypeptides in the ATP-dependent proteasome (20); the increase of proteolysis in MDKO muscle therefore contributes to the depletion of energy stores. Second, the lack of insulin signaling in MDKO muscle likely impairs mitochondrial oxidative phosphorylation and ATP production, as previously seen in hepatocytes lacking both Irs1 and Irs2 (9). Consistent with this, deletion of Ir and Igf1r using MCK-Cre decreases expression of mitochondrial electron transport chain genes in cardiac muscle (35). Third, elevated lactate release from MDKO skeletal muscle diminishes pyruvate availability for the synthesis of oxaloacetate—a critical anaplerotic pathway to replenish the TCA cycle (47) (Fig. 7); thus, the efficiency of coupling fatty acid oxidation to the TCA cycle for energy production is also likely compromised. Collectively, these perturbations increase the energy demand and impair energy production in MDKO skeletal muscle, resulting in a sustained increase in the AMP/ATP ratio that is uncompensated by AMPK activation.

As previously reported for the deletion of muscle insulin and IGF1 receptors by MCK-Cre (35) and also for the cardiac muscle-specific deletion of Irs1 and Irs2 (49), our MDKO mice exhibit dilated cardiomyopathy. However, it appears likely that the skeletal muscle growth and metabolic phenotypes that we observe in 2-week-old MDKO mice are largely independent of this cardiac pathology. First, the presence of milk in the stomachs of MDKO pups during necropsy revealed that these mice suckled normally. Second, excepting the skeletal muscles, the masses of all investigated organs and tissues in MDKO mice (including the heart, where MCK-Cre was active) were unaltered. Most importantly, cardiomyocyte-specific disruption of Irs1 and Irs2 expression causes a similar early lethal phenotype in mice, but without overt derangement of systemic metabolism (E. D. Abel, personal communication) (49).

By restoring Irs1 or Irs2 expression in cardiac muscle with an appropriate transgene, it might be possible to extend the life span of MDKO mice significantly; such an approach would facilitate investigation of the progression of systemic insulin action and glucose tolerance as the mice age into adults. Transgenic mice with a skeletal muscle-specific dominant-negative IGF1 receptor develop impaired muscle glucose uptake in response to IGF1 and insulin and hyperinsulinemia, with glucose and insulin intolerance (37). Owing to the formation of hybrid receptors, the dominant-negative IGF1 receptor apparently inhibits both IGF1 and insulin receptor signaling. It will be important to establish whether adult mice without skeletal muscle Irs1 and Irs2 signaling can maintain glucose tolerance through the alternative metabolism described in this report.

In summary, insulin-like signaling mediated by Irs1 and Irs2 activates the Akt→mTOR signaling cascade and inhibits Foxo pathways, which reciprocally regulate skeletal muscle growth/atrophy (Fig. 7). An increased AMP/ATP ratio, coincident with the increased metabolism of glucose to lactate in MDKO muscle, activates AMPK. Increased AMPK activity further antagonizes mTOR/Raptor-mediated protein synthesis while failing to completely restore the energy balance via upregulation of fatty acid oxidation. Thus, insulin-like signals mediated by Irs1/2 are essential to coordinate nutrient availability with skeletal muscle growth to maintain whole-body metabolic homeostasis.

ACKNOWLEDGMENTS

This work was supported by a grant from the National Institutes of Health (DK38712) and the Howard Hughes Medical Institute.

REFERENCES

1. **Abbud, W., et al.** 2000. Stimulation of AMP-activated protein kinase (AMPK) is associated with enhancement of Glut1-mediated glucose transport. Arch. Biochem. Biophys. **380:**347–352.
2. **Araki, E., et al.** 1994. Alternative pathway of insulin signalling in mice with targeted disruption of the IRS-1 gene. Nature **372:**186–190.
3. **Barnes, B. R., et al.** 2005. 5′-AMP-activated protein kinase regulates skeletal muscle glycogen content and ergogenics. FASEB J. **19:**773–779.
4. **Barnes, K., et al.** 2002. Activation of GLUT1 by metabolic and osmotic stress: potential involvement of AMP-activated protein kinase (AMPK). J. Cell Sci. **115:**2433–2442.
5. **Bassel-Duby, R., and E. N. Olson.** 2006. Signaling pathways in skeletal muscle remodeling. Annu. Rev. Biochem. **75:**19–37.
6. **Bastie, C. C., et al.** 2005. FoxO1 stimulates fatty acid uptake and oxidation

in muscle cells through CD36-dependent and -independent mechanisms. J. Biol. Chem. **280:**14222–14229.
7. **Bentzinger, C. F., et al.** 2008. Skeletal muscle-specific ablation of raptor, but not of rictor, causes metabolic changes and results in muscle dystrophy. Cell Metab. **8:**411–424.
8. **Bruning, J. C., et al.** 1998. A muscle-specific insulin receptor knockout exhibits features of the metabolic syndrome of NIDDM without altering glucose tolerance. Mol. Cell **2:**559–569.
9. **Cheng, Z., et al.** 2009. Foxo1 integrates insulin signaling with mitochondrial function in the liver. Nat. Med. **15:**1307–1311.
10. **Cho, H., et al.** 2001. Insulin resistance and a diabetes mellitus-like syndrome in mice lacking the protein kinase Akt2 (PKB beta). Science **292:**1728–1731.
11. **Copps, K. D., et al.** 2010. Irs1 serine 307 promotes insulin sensitivity in mice. Cell Metab. **11:**84–92.
12. **Cross, D. A. E., et al.** 1997. Insulin activates protein kinase B, inhibits glycogen synthase kinase-3 and activates glycogen synthase by rapamycin-insensitive pathways in skeletal muscle and adipose tissue. Growth Regul. **406:**211–215.
13. **Dong, X. C., et al.** 2008. Inactivation of hepatic Foxo1 by insulin signaling is required for adaptive nutrient homeostasis and endocrine growth regulation. Cell Metab. **8:**65–76.
14. **Frayn, K. N.** 2003. The glucose-fatty acid cycle: a physiological perspective. Biochem. Soc. Trans. **31**(Pt. 6)**:**1115–1119.
15. **Fujii, N., N. Jessen, and L. J. Goodyear.** 2006. AMP-activated protein kinase and the regulation of glucose transport. Am. J. Physiol. Endocrinol. Metab. **291:**E867–E877.
16. **Furuyama, T., K. Kitayama, H. Yamashita, and N. Mori.** 2003. Forkhead transcription factor FOXO1 (FKHR)-dependent induction of PDK4 gene expression in skeletal muscle during energy deprivation. Biochem. J. **375:** 365–371.
17. **Garofalo, R. S., et al.** 2003. Severe diabetes, age-dependent loss of adipose tissue, and mild growth deficiency in mice lacking Akt2/PKB beta. J. Clin. Invest. **112:**197–208.
18. **Gazdag, A. C., C. L. Dumke, C. R. Kahn, and G. D. Cartee.** 1999. Calorie restriction increases insulin-stimulated glucose transport in skeletal muscle from IRS-1 knockout mice. Diabetes **48:**1930–1936.
19. **Glass, D. J.** 2003. Signalling pathways that mediate skeletal muscle hypertrophy and atrophy. Nat. Cell Biol. **5:**87–90.
20. **Goldberg, A. L.** 2007. Functions of the proteasome: from protein degradation and immune surveillance to cancer therapy. Biochem. Soc. Trans. **35:** 12–17.
21. **Greer, E. L., M. R. Banko, and A. Brunet.** 2009. AMP-activated protein kinase and FoxO transcription factors in dietary restriction-induced longevity. Ann. N. Y. Acad. Sci. **1170:**688–692.
22. **Guo, S., et al.** 2009. The Irs1 branch of the insulin signaling cascade plays a dominant role in hepatic nutrient homeostasis. Mol. Cell. Biol. **29:**5070–5083.
23. **Gwinn, D. M., et al.** 2008. AMPK phosphorylation of raptor mediates a metabolic checkpoint. Mol. Cell **30:**214–226.
24. **Higaki, Y., et al.** 1999. Insulin receptor substrate-2 is not necessary for insulin- and exercise-stimulated glucose transport in skeletal muscle. J. Biol. Chem. **274:**20791–20795.
25. **Howlett, K. F., et al.** 2002. Insulin signaling after exercise in insulin receptor substrate-2-deficient mice. Diabetes **51:**479–483.
26. **Huang, J., and B. D. Manning.** 2008. The TSC1-TSC2 complex: a molecular switchboard controlling cell growth. Biochem. J. **412:**179–190.
27. **Kahn, B. B., T. Alquier, D. Carling, and D. G. Hardie.** 2005. AMP-activated protein kinase: ancient energy gauge provides clues to modern understanding of metabolism. Cell Metab. **1:**15–25.
28. **Kamei, Y., et al.** 2004. Skeletal muscle FOXO1 (FKHR) transgenic mice have less skeletal muscle mass, down-regulated type I (slow twitch/red muscle) fiber genes, and impaired glycemic control. J. Biol. Chem. **39:**41114–41123.
29. **Karlsson, H. K., and J. R. Zierath.** 2007. Insulin signaling and glucose transport in insulin resistant human skeletal muscle. Cell Biochem. Biophys. **48:**103–113.
30. **Kelley, D. E.** 2005. Skeletal muscle fat oxidation: timing and flexibility are everything. J. Clin. Invest. **7:**1699–1702.
31. **Kubota, N., et al.** 2008. Dynamic functional relay between insulin receptor substrate 1 and 2 in hepatic insulin signaling during fasting and feeding. Cell Metab. **8:**49–64.
32. **Kumar, A., et al.** 2008. Muscle-specific deletion of rictor impairs insulin-stimulated glucose transport and enhances basal glycogen synthase activity. Mol. Cell. Biol. **28:**61–70.
33. **Laplante, M., and D. M. Sabatini.** 2009. mTOR signaling at a glance. J. Cell Sci. **122:**3589–3594.
34. **Latres, E., et al.** 2005. Insulin-like growth factor-1 (IGF-1) inversely regulates atrophy-induced genes via the phosphatidylinositol 3-kinase/Akt/mammalian target of rapamycin (PI3K/Akt/mTOR) pathway. J. Biol. Chem. **280:** 2737–2744.
35. **Laustsen, P. G., et al.** 2007. Essential role of insulin and insulin-like growth factor 1 receptor signaling in cardiac development and function. Mol. Cell. Biol. **27:**1649–1664.
36. **Lecker, S. H., A. L. Goldberg, and W. E. Mitch.** 2006. Protein degradation by the ubiquitin-proteasome pathway in normal and disease states. J. Am. Soc. Nephrol. **17:**1807–1819.
37. **Leroith, D., and D. Accili.** 2008. Mechanisms of disease: using genetically altered mice to study concepts of type 2 diabetes. Nat. Clin. Pract. Endocrinol. Metab. **4:**164–172.
38. **Lin, X., et al.** 2004. Dysregulation of insulin receptor substrate 2 in beta cells and brain causes obesity and diabetes. J. Clin. Invest. **114:**908–916.
39. **Long, Y. C., and J. R. Zierath.** 2006. AMP-activated protein kinase signaling in metabolic regulation. J. Clin. Invest. **116:**1776–1783.
40. **Mammucari, C., et al.** 2007. FoxO3 controls autophagy in skeletal muscle in vivo. Cell Metab. **6:**458–471.
41. **Mammucari, C., S. Schiaffino, and M. Sandri.** 2008. Downstream of Akt: FoxO3 and mTOR in the regulation of autophagy in skeletal muscle. Autophagy **4:**524–526.
42. **Masiero, E., et al.** 2009. Autophagy is required to maintain muscle mass. Cell Metab. **10:**507–515.
43. **McCurdy, C. E., and G. D. Cartee.** 2005. Akt2 is essential for the full effect of calorie restriction on insulin-stimulated glucose uptake in skeletal muscle. Diabetes **54:**1349–1356.
44. **Miyamoto, L., et al.** 2007. Effect of acute activation of 5′-AMP-activated protein kinase on glycogen regulation in isolated rat skeletal muscle. J. Appl. Physiol. **102:**1007–1013.
45. **Morino, K., K. F. Petersen, and G. I. Shulman.** 2006. Molecular mechanisms of insulin resistance in humans and their potential links with mitochondrial dysfunction. Diabetes **55**(Suppl. 2)**:**S9–S15.
46. **Obsil, T., and V. Obsilova.** 2008. Structure/function relationships underlying regulation of FOXO transcription factors. Oncogene **27:**2263–2275.
47. **Owen, O. E., S. C. Kalhan, and R. W. Hanson.** 2002. The key role of anaplerosis and cataplerosis for citric acid cycle function. J. Biol. Chem. **277:**30409–30412.
48. **Petersen, K. F., et al.** 2007. The role of skeletal muscle insulin resistance in the pathogenesis of the metabolic syndrome. Proc. Natl. Acad. Sci. U. S. A. **104:**12587–12594.
49. **Riehle, C., et al.** 2008. Insulin receptor substrates (IRS) signaling are essential regulators of mitochondrial function and cardiomyocyte survival. Circulation **118:**S444. (Abstract.)
50. **Ruderman, N. B.** 1975. Muscle amino acid metabolism and gluconeogenesis. Annu. Rev. Med. **26:**245–258.
51. **Sacheck, J. M., A. Ohtsuka, S. C. McLary, and A. L. Goldberg.** 2004. IGF-I stimulates muscle growth by suppressing protein breakdown and expression of atrophy-related ubiquitin ligases, atrogin-1 and MuRF1. Am. J. Physiol. Endocrinol. Metab. **287:**E591–E601.
52. **Sandri, M., et al.** 2004. Foxo transcription factors induce the atrophy-related ubiquitin ligase atrogin-1 and cause skeletal muscle atrophy. Cell **117:**399–412.
53. **Savage, D. B., K. F. Petersen, and G. I. Shulman.** 2007. Disordered lipid metabolism and the pathogenesis of insulin resistance. Physiol. Rev. **87:**507–520.
54. **Spargo, E., O. E. Pratt, and P. M. Daniel.** 1979. Metabolic functions of skeletal muscles of man, mammals, birds and fishes: a review. J. R. Soc. Med. **12:**921–925.
55. **Taguchi, A., and M. F. White.** 2008. Insulin-like signaling, nutrient homeostasis, and life span. Annu. Rev. Physiol. **70:**191–212.
56. **Takata, M., et al.** 1999. Requirement for Akt (protein kinase B) in insulin-induced activation of glycogen synthase and phosphorylation of 4E-BP1 (PHAS-1). J. Biol. Chem. **274:**20611–20618.
57. **Tamemoto, H., et al.** 1994. Insulin resistance and growth retardation in mice lacking insulin receptor substrate-1. Nature **372:**182–186.
58. **Winder, W. W.** 2001. Energy-sensing and signaling by AMP-activated protein kinase in skeletal muscle. J. Appl. Physiol. **91:**1017–1028.
59. **Winder, W. W., et al.** 1997. Phosphorylation of rat muscle acetyl-CoA carboxylase by AMP-activated protein kinase and protein kinase A. J. Appl. Physiol. **82:**219–225.
60. **Zhao, J., et al.** 2007. FoxO3 coordinately activates protein degradation by the autophagic/lysosomal and proteasomal pathways in atrophying muscle cells. Cell Metab. **6:**472–483.
61. **Zhao, J., J. J. Brault, A. Schild, and A. L. Goldberg.** 2008. Coordinate activation of autophagy and the proteasome pathway by FoxO transcription factor. Autophagy **3:**378–380.
62. **Zisman, A., et al.** 2000. Targeted disruption of the glucose transporter 4 selectively in muscle causes insulin resistance and glucose intolerance. Nat. Med. **6:**924–928.